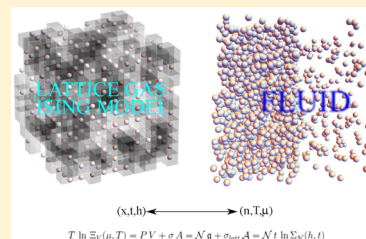


Surface Tension of the Liquid–Vapor Interface of the Lennard-Jones Fluids from the Ising Model

V. L. Kulinskii*[†] and A. Maslechko[‡][†]Department of Theoretical Physics, Odessa National University, Dvoryanskaya 2, 65082 Odessa, Ukraine[‡]Department of Chemistry, Norwegian University of Science and Technology, Hogskoleringen 5, N-7491 Trondheim, Norway

ABSTRACT: The surface tension of the Lennard-Jones fluids is described on the basis of the information about Ising model. We use the global isomorphism approach developed earlier for the bulk properties. It is shown that in broad interval of phase coexistence from triple point T_{tr} to $0.9 T_c$ the surface tension for Lennard-Jones fluids like noble gases can be reproduced on the basis of the information on the Ising model with mean deviation less than 3% (except for neon). In a 2D case, we use the Onsager exact solution of the Ising model. We suggest the surface tension expression using the result of Woodbury (*J. Chem. Phys.* **1972**, *57*, 847). This expression has correct critical scaling behavior and can be used in the whole temperature region from triple point to critical one. The effective interfacial thickness is introduced on the basis of the Ornstein–Zernike equation and is related to the correlation length of the Ising model.



■ INTRODUCTION

Lattice models play an important role in our understanding of the behavior of the real systems which are too complex to be treated in a controllable way. In general discrete models are used independently, therefore a direct comparison between different systems is impossible. Situations where the physical quantities of different models or substances can be related are of great interest. The principle of corresponding states (PCS) plays an important role here.^{1,2} The PCS as the global statement about the phase diagram of some class of substances which have similar thermodynamic properties is the guide in searching simple empirical laws in reduced variables.

One of these laws is the (approximate) rectilinear density diameter law:

$$n_d = \frac{n_l + n_g}{2n_c} = 1 + A(1 - T/T_c) \quad (1)$$

where T is the temperature, n_{lg} are the densities of the liquid and vapor phases, correspondingly, and n_c and T_c are the critical density and the temperature. It has been known more than a century since the work of Cailletet and Mathias.³ It is explicitly used in the famous Guggenheim equation of state for simple fluids.⁴ Because of that, the relation in eq 1 can be used for targeting the critical point in computer simulations.⁵ The deviations from linearity in eq 1 is noticeable in mercury where the interaction varies with the thermodynamic state⁶ and is noticeable in water because of the nonmonotonic behavior of the thermal expansion coefficient. Nevertheless, eq 1 can serve as a good approximation in the whole region of vapor–liquid coexistence excluding close vicinity of the critical point.

Another important empirical linearity is the Zeno line (ZL) linearity⁷ which states the linear temperature behavior for the n – T line determined by the unit compressibility value:

$$Z = \frac{P}{nT} \Rightarrow \frac{T}{T_Z} + \frac{n}{n_Z} = 1 \quad (2)$$

The latter is fulfilled trivially for the van der Waals equation and is known as the Batschinski law.⁸ Here T_Z and n_Z are determined via virial coefficients:⁷

$$B_2(T_Z) = 0, \quad n_Z = \frac{T_Z}{B_3(T_Z)} \frac{dB_2}{dT} \Big|_{T=T_Z} \quad (3)$$

Recently, in a series of works by Apfelbaum and Vorob'ev^{9–11} it was pointed out that this linearity holds for broad class of molecular fluids and liquid metals.

In works of Kulinskii et al.^{12–14} the global isomorphism approach was introduced and applied to the study of bulk properties of the Lennard-Jones fluids. This approach is based on the topological equivalence between phase diagram of the Ising model and the liquid–vapor diagram for the class of fluids for which the linearities (eqs 1, 2) hold empirically with good accuracy.

The lattice gas (LG) representation of the Ising model is given by the Hamiltonian (see, e.g., ref 15):

$$H_{LG} = -\varepsilon \sum_{(i,j)} n_i n_j - \mu \sum_i n_i \quad (4)$$

There is the nearest cite–cite attraction with the energy ε , the repulsive part is modeled by the restriction for the occupation number of a cite $n_i = 0, 1$, and μ is the chemical potential. Note that in case of the Ising model, the RLD (1) is fulfilled trivially because of the spin-flop symmetry. In that case the Zeno-line

Received: February 28, 2016

Revised: March 27, 2016

Published: April 6, 2016

analog is the line $x = 1$ where x is the molar part $x = N/N$ of N occupied sites in a lattice with total N sites.

The class of fluids which obey the above-mentioned linearities includes systems with the Lennard-Jones (LJ) potential as well as other generalized Mie-potential and Yukawa fluids as well as fluids with square well potential.^{16–18} In such case simple geometrical transformation between thermodynamic states of fluid and lattice systems can be constructed (see^{12,13}):

$$n(x, \tilde{t}) = n_* \frac{x}{1 + z\tilde{t}}, \quad T(\tilde{t}) = T_* \frac{z\tilde{t}}{1 + z\tilde{t}} \quad (5)$$

with

$$z = \frac{T_c}{T_* - T_c}$$

The inverse transformation is

$$x = \frac{n}{n_*} \frac{T_*}{T_* - T}, \quad \tilde{t} = \frac{1}{z} \frac{T}{T_* - T} \quad (6)$$

Here, \tilde{t} is the temperature variable of the LG model normalized by its critical temperature value t_c : $\tilde{t} = t/t_c$. The parameters T_* and n_* of a linear Zeno-element:

$$\frac{n}{n_*} + \frac{T}{T_*} = 1 \quad (7)$$

are determined via the Boyle point in van der Waals (vdW) approximation (see, e.g., ref 19):

$$B_2^{vdW}(T_*) = 0, \quad T_* = T_Z^{(vdW)} = \frac{a}{b} \quad (8)$$

with

$$a = -2\pi \int_d^{+\infty} \Phi_{attr}(r) r^2 dr \quad (9)$$

Here $\Phi_{attr}(r)$ is the attractive part of the interaction potential $\Phi(r)$, d is the diameter of the particle so that $b = \frac{2\pi}{3} d^3$. The density parameter n_* represents the high density state with $n_* \approx 1/b$:

$$n_* = \frac{T_*}{B_3(T_*)} \frac{dB_2}{dT} \Big|_{T=T_*} \quad (10)$$

The parameter z is related to the scaling properties of the Hamiltonian (eq 4) and in particular to its asymptotic attractive part $\propto r^{-6}$ of the LJ potential:¹³

$$\Phi_{LJ}(r) = 4\Phi_0 \left(\left(\frac{d}{r} \right)^{12} - \left(\frac{d}{r} \right)^6 \right) \quad (11)$$

as follows

$$z = \frac{6}{D} \quad (12)$$

where D is the spatial dimension.¹³ For the LJ-fluid, we use conventional dimensionless units for the temperature $T \rightarrow T/\Phi_0$, density $n \rightarrow nd^3$, and pressure $P \rightarrow Pd^3/\Phi_0$. The relation between the LJ parameter Φ_0 , lattice gas interaction ε in eq 4 and the spin–spin interaction J of the Ising model does not depend on the spatial dimension and is as follows (see, e.g., refs 15 and 20):

$$\Phi_0 = \varepsilon = 4J \quad (13)$$

In 2D and 3D cases for the LJ “6–12”-potential $T_* = 2\varepsilon$ and $T_* = 4\varepsilon$.¹³ We use eq 13 as the test mark below.

The subject of the paper is to relate the surface tensions of the lattice gas (Ising model) and the LJ fluid. The results obtained for the binodal in^{14,21} give the ground to apply the developed approach to the surface tension since from the thermodynamic point of view this physical quantity is the thermodynamic potential of the surface.²²

We review some results of the global isomorphism approach for the bulk properties and extend it to the surface tension. We use the result of work²³ to construct the surface tension using the bulk properties (densities of the coexisting liquid and gas phases). Our core result is the modified Woodbuty's expression in the simplest Bragg–Williams approximation. The definition of the interfacial thickness using the Ornstein–Zernike equation is given. The consequences are checked for 2D and 3D cases using available data. The results are summarized in the **Conclusion**, where also some problems for prospective studies are noted.

■ GLOBAL ISOMORPHISM FLUID–LATTICE GAS FOR THE BULK AND SURFACE PROPERTIES

In ref 14, it was shown that the transformations (eq 5) can be derived from the following relation between the bulk thermodynamic potentials of the LJ fluid and the lattice gas:

$$\Psi = P(\mu(h), T(t))V = \mathcal{G}(h, t) = \mathcal{N}g(h, t) \quad (14)$$

Here Ψ and \mathcal{G} are the Gibbsian potentials of the fluid and the lattice gas (Ising model) correspondingly, P is the pressure and μ is the chemical potential of the LJ fluid, V - its volume, h is the field variable conjugated to x , \mathcal{N} is the number of sites of the LG. Indeed, taking into account the relationship between the temperature variables t and T using the thermodynamic relations:

$$n = \frac{\partial P}{\partial \mu} \Big|_T, \quad x = \frac{\partial g}{\partial h} \Big|_t \quad (15)$$

it is easy to get the relation between the densities n and x . On this basis,^{24,25} the following relation between critical compressibility factors of these systems was obtained:

$$Z_c^{(fl)} = \frac{P_c}{n_c T_c} = \frac{(1+z)^2}{z} \frac{t_c}{T_*} Z_c^{(LG)} \quad (16)$$

where $Z_c^{(LG)}$ is the critical compressibility factor of the LG. The latter is related with the partition function per spin $G^{1/N}$ of the Ising model $Z_c^{(LG)} = 2 \ln G_c^{1/N}$. In the 3D, case $t_c \approx 4.51 J^{26}$ and $Z_c^{(LG)} = 0.221$ for cubic lattice,²⁷ which leads to

$$Z_c^{(fl)} \approx 1.27 Z_c^{(LG)} = 0.281 \quad (17)$$

This value agrees with known result for the value of 3D LJ fluid and real data for the noble fluids like Ar, Kr, Xe with $Z_c \approx 0.29$, which obviously fall into the same class of thermodynamic similarity. In this way it is possible to explain the results of work.²⁸ The authors demonstrated, that for classical molecular fluids, as well as helium, hydrogen, and neon, the fugacity value

$$\zeta = e^{\mu(P,T) - \mu_{id}(P,T)/T} \quad (18)$$

at the critical point takes the universal value $\zeta_c = 1.51 \pm 0.01$. Note that for the same class of fluids they reported $Z_c = 0.276 \pm 0.009$ which is consistent with the Ising-like value (eq 17). So both the universality Z_c and ζ_c have the same nature within the

global isomorphism approach. The specific value of ζ can be obtained on the basis of the information available for the Ising model, in a similar way we did for Z_c above (see eq 16).

These results indicate that the global isomorphism is valid for the bulk properties. In particular, the relation 14 can be used as the starting point to relate the interfacial properties of these systems. A consideration of the thermodynamics with account of surface contribution is much more difficult because of the inhomogeneity.^{29,30} Nevertheless, we can extend the relation 14 to account for the surface tension term (we put $k_B = 1$):

$$\begin{aligned} T \ln \Xi_V(\mu, T) &= PV + \sigma A = \mathcal{N}g + \sigma_{latt} \mathcal{A} \\ &= \mathcal{N}t \ln \Sigma_{\mathcal{N}}(h, t) \end{aligned} \quad (19)$$

where $\Xi_V(\mu, T)$ and $\Sigma_{\mathcal{N}}(h, t)$ are corresponding partition functions for the ensembles, σ and σ_{latt} - the surface tensions and A is the total area of interfacial surface, g is the Gibbs energy per site in LG. The surface tension in lattice models is due to the following representation of the partition function:

$$\Sigma_{\mathcal{N}}^{(latt)} = \Lambda_{max}^{m_2} + \Lambda_1^{m_2} + \dots \quad (20)$$

where $\mathcal{N} = m_1 \times m_2$ is the size of the lattice, Λ_{max} , Λ_1 are the maximal and the next eigenvalues of the transfer-matrix correspondingly.¹⁵ In cases where no exact analytical solution is available for the LG one may use the results of works.^{31,32} There it was shown that the surface tension in the lattice models can be expressed as the difference between averages of the local physical quantity in coexisting phases:

$$\sigma_{latt} = t(\langle s \rangle_{gas} - \langle s \rangle_{liq}) \quad (21)$$

Here s is the local variable which corresponds to the spin distribution in the slice far from the interface. E.g. in the simplest Bragg-Williams approximation s is reduced to

$$s \approx \frac{1}{2} \sum_i \ln p(s_i) \quad (22)$$

where $p(s_i)$ is a distribution of the i th spin in the slice. Due to the symmetry between the coexisting phases

$$x_{gas} = 1 - x_{liq} = \frac{1 - m}{2}, \quad m = \langle s \rangle$$

the substitution of eq 22 into eq 21 leads to

$$\sigma_{latt}(t) = \frac{t}{2l_0^{D-1}} (x_{liq} - x_{gas}) \ln \frac{x_{liq}}{x_{gas}} \quad (23)$$

Here l_0 is the lattice spacing.²³ Further we put $l_0 = 1$ (in dimensionless units) for simplicity. Neglecting the correlations leads to very crude approximation, especially in the fluctuation region. There the direct comparison of eq 21 with known values of the surface tension gave inadequate difference between the theoretical prediction and experimental data.²³ In order to correct this inconsistency yet to conserve analytical simplicity for the functional dependence of the s on x , we modify eq 23. To do this we analyze the contribution to the critical behavior of the surface tension from the basic expressions of statistical mechanics in the following section.

Note that the result (eq 21) has its analogue in case of fluid systems. Indeed, mechanical definition of the surface tension is

$$\sigma = \int_{-\infty}^{\infty} (P - P_{\tau}(z)) dz \quad (24)$$

where P_{τ} is tangential component of the pressure.³³ Limits of integration correspond to homogeneous phases and therefore ultimately the integral is a difference of the bulk quantities:

$$\sigma = \Pi(+\infty) - \Pi(-\infty) \quad (25)$$

where

$$\Pi(z) = Pz - \int_0^z P_{\tau}(x) dx \quad (26)$$

The limits in eq 25 may be reduced to some characteristic length ξ_{eff} . We call it the effective thickness of the surface and define it in following section. Its temperature dependence should resemble the behavior of the correlation length. In particular, such effective thickness diverges at the critical point with the critical exponent ν of correlation length.^{34,35}

Taking into account the relation 5 between densities in eq 23, we get the following density dependence of the surface tension of the LJ fluid:

$$\sigma \propto (n_{liq} - n_{gas})^2 \quad (27)$$

near the critical point where n_{liq} and n_{gas} are close to each other. This relation is in accordance with the result of^{36,37} obtained on the basis of the classical Kirkwood–Buff formula for the surface tension. Note that in comparison with the Parachore approach³⁸

$$\sigma = C(n_l - n_g)^a, \quad a \approx 3.55 \quad (28)$$

which is widely used for the surface tension data processing (see, e.g., refs 39 and 40) the expression 21 depends not only on the density difference $n_l - n_g$ on the binodal but also on the binodal diameter (eq 1). Though the Parachore expression eq 28 looks very simple it seems that it can not be justified on the basis of the exact Kirkwood–Buff formula for the surface tension. Moreover, as we will see below in 2D case the surface tension for the lattice model does not have simple scaling form of eq 28. In the following section, we demonstrate how eq 21 can be modified on the basis of the Trietzenberg–Zwanzig formula⁴¹ which is known to be equivalent to the Kirkwood–Buff expression.

■ MODIFIED WOODBURY'S EXPRESSION AND THE EFFECTIVE WIDTH OF THE INTERFACE

To find simple modification of the Woodbury expression, eq 21, consistent with the critical asymptotic we use the Trietzenberg–Zwanzig formula⁴¹

$$\sigma = T \iint dn(z_1) dn(z_2) K_2(z_1, z_2) \quad (29)$$

As is known eq 29 is equivalent to the Kirkwood–Buff expression.⁴² Here

$$K_2(z_1, z_2) = \frac{1}{4} \int d^{D-1} \rho \rho^2 C_2(z_1, z_2; \rho) \quad (30)$$

$\rho = (x, y)$ is the vector along planar interface and C_2 is the direct correlation function for corresponding inhomogeneous state. Note that the square gradient van der Waals approximation

$$\sigma_{vdW} = \frac{b}{2} \int_{-\infty}^{+\infty} \left(\frac{dn(z)}{dz} \right)^2 dz \quad (31)$$

with $b = \text{const}$, which follows from (eq 29) in local approximation for the kernel $K_2 \sim \delta(z_1 - z_2)$, leads to inaccurate critical asymptotic $\sigma_{vdW} \propto |\tau|^{2\beta-\nu}$.

Near the critical point the density profile can be represented as follows:

$$n_1(z) = n_0 - \frac{\Delta n}{2} f(z/\xi), \quad n_0 = \frac{1}{2}(n_l + n_g) \quad (32)$$

where $\Delta n = n_l - n_g$ with $\Delta n \sim \tau^\beta$ and the profile function has the following asymptotes:

$$f(z) \rightarrow \begin{cases} +1, & z \rightarrow +\infty \\ -1, & z \rightarrow -\infty \end{cases}$$

Note that the main contribution to the criticality of the surface tension in eq 29 is due to the symmetric part of the function C_2 . Since the surface tension σ vanishes at the critical point its critical behavior is governed by the excessive (over the critical value) part of C_2 . Using the standard relation:

$$\frac{1}{T} \left(\frac{\partial p}{\partial n} \right)_T = 1 - n \int C_2(n; \mathbf{r}_{12}) d\mathbf{r}_{12} \quad (33)$$

and the critical asymptotic $\frac{\partial p}{\partial n}|_T \propto |\tau|^\gamma$, for the excessive part of C_2 from eq 33 we get:

$$C_2^{(ex)}(n; \mathbf{r}_{12}) \propto |\tau|^{2-\alpha+\gamma} \propto \frac{1}{\xi^{D+2-\eta}} \quad (34)$$

It is assumed that the characteristic size of integration region in eq 33 is of order of the correlation length ξ at least in the vicinity of the critical point. Therefore, in the leading order K_2 scales as

$$K_2(z_1, z_2) = \frac{1}{4} \int d^{D-1} \rho \rho^2 C_2(z_1, z_2; \rho) \propto \frac{\xi^{D+1}}{\xi^{D+2-\eta}} \propto \frac{1}{\xi^{1-\eta}} \quad (35)$$

which contributes to the critical asymptotics of the surface tension. Substitution of this result into eq 29 yields to the standard scaling result for σ :

$$\sigma \propto \frac{\Delta n^2}{\xi^{1-\eta}} \propto |\tau|^{2\beta+\nu(1-\eta)} = |\tau|^{(D-1)\nu} \quad (36)$$

In the case of a fluid, there is uncertainty in the determination of ξ because there are two correlation lengths of the bulk phases as well as the width of the interface itself. In Ising model two bulk correlation lengths coincide due to the ‘‘particle-hole’’ symmetry. Taking this into account we modify the Woodbury formula as follows:

$$\sigma_{latt} = \frac{\sigma_0}{2} \frac{t}{\xi_{eff}^{1-\eta}} (1 - 2x_{gas}) \ln \frac{1 - x_{gas}}{x_{gas}} \quad (37)$$

Here the length ξ_{eff} can be treated as the effective thickness of the interface in units of molecular size. Further we use the dimensionless units for length scale in units of molecular diameter. The amplitude factor σ_0 is determined by matching some reference point and further will be used as a fitting parameter. Expression 37 has the correct critical asymptote for the surface tension $\sigma \propto |\tau|^{(D-1)\nu}$ provided that the effective thickness of the surface behaves as $\xi_{eff} \propto |\tau|^{-\nu}$. Formula 37 can be used to obtain the surface tension of the LJ fluid, if we augment it by the global isomorphism relations (eq 5). So eq 37 satisfies asymptotic behavior which follows from the fluctuation theory and is coherent with the statistical mechanics formulas for the surface tension. The value of ξ_{eff} is of the order of the correlation length.³⁴ It can be estimated via the density profile $n(z)$ on the basis of widely used ‘‘10–90’’ rule. In fact the value

of interfacial thickness depends on its definition and approximations for the pair correlation function used (see, e.g., ref 43).

Now let us try to define the width of the interface as the characteristic of the density profile from the basics of liquid state theory. We consider the Ornstein–Zernike (OZ) relation between the full and direct pair correlation functions G_2 and C_2 correspondingly in inhomogeneous state:²⁹

$$G_2(\mathbf{1}, \mathbf{2}) = C_2(\mathbf{1}, \mathbf{2}) + \int C_2(\mathbf{1}, \mathbf{3}) G_2(\mathbf{3}, \mathbf{2}) n(\mathbf{3}) d\mathbf{3} \quad (38)$$

Introducing the operator form of eq 38

$$\hat{G}_2 = \hat{C}_2 + \hat{Q}[n] \quad (39)$$

Here the operator \hat{Q} is as following

$$\hat{Q} = \hat{C}_2 \star \hat{G}_2$$

where \star stands for the convolution. In homogeneous case of the only bulk phase with uniform equilibrium density $n_{eq} = 1/v_{eq}$ the OZ relation can be treated as the relation between some specific volumes defined by the full and direct correlation functions:

$$\frac{1}{\tilde{C}_2(\mathbf{k})} = \frac{1}{\tilde{G}_2(\mathbf{k})} + 1/v_{eq} \quad (40)$$

simply because of dimension reasonings. Note that for molecular fluids in the vicinity of the critical point G_2 is long ranged and C_2 is short ranged functions correspondingly.²⁹

In case of the planar geometry only z -dependence perpendicular to the plane surface is relevant and therefore the OZ relation can be rewritten as the relation between some characteristic scales related with corresponding correlation functions. Therefore, we can write the formal inverse form of eq 39:

$$\hat{Q}^{-1} \hat{G}_2 = n(z) + \hat{Q}^{-1} \hat{C}_2 \quad (41)$$

In order to define the length scale connected with the width of the interface from eq 41 we derive:

$$\int \partial_z \hat{Q}^{-1} \hat{G}_2 dV = \int \partial_z n dV + \int \partial_z \hat{Q}^{-1} \hat{C}_2 dV \quad (42)$$

Obviously, all terms have the dimension of inverse length. We note that the density term and the quantity:

$$\Lambda = \int \partial_z (\hat{Q}^{-1} \hat{C}_2) dV$$

has the same local character as Λ is determined by the spatial behavior of the direct correlation function which can be seen from the comparison with eq 40. Their difference varies at larger scale which is identified with the characteristic length of the full correlation function term in eq 42. Then eq 42 can be rewritten in an equivalent form:

$$1 = \Lambda^{-1} \int \partial_z n dV + \Lambda^{-1} \int \partial_z (\hat{Q}^{-1} \hat{C}_2) dV \quad (43)$$

As has been noted above the first term in eq 43 can be associated with ξ_w as it is determined by the long ranged correlation function:

$$\xi_w^{-1} = \Lambda^{-1} \int \partial_z (\hat{Q}^{-1} \hat{C}_2) dV$$

The latter, of course, determines the characteristic interfacial width which diverges at the critical point the same way as the correlation length does. The other term

$$\xi_0^{-1} = \Lambda^{-1} \int \partial_z n \, dV$$

represents “dual” microscopic length scale which is related to the direct correlation function C_2 as it remains short ranged even at the critical point and its integral over the distance is determined by the density. Thus, eq 43 takes the form

$$\frac{1}{\xi_0(T)} + \frac{1}{\xi_w(T)} = 1 \quad (44)$$

where all lengths are dimensionless in terms of molecular size. Clearly, it is assumed that $\xi_0(T_c) = 1$ as $\xi_{eff}(T_c) \rightarrow \infty$ and $\xi_w(T) > (\gg) 1$. From physical point of view one can expect that for fluid systems $\xi_w(T) > \xi_0(T)$ since ξ_0 is related with the direct correlation function spacial behavior which is short ranged. Taking into account monotonic decrease of the interfacial width ξ_w for simple fluids where orientational correlations rather weak it is possible to derive the lower estimate for the triple point temperature T_{tr} basing on the inequality:

$$\xi_w(T_{tr}) \geq 2 \quad (45)$$

The proposed definition for the interfacial width does not depend on the arbitrariness of the “ $p/(1-p)$ ” rule or the specific exponential factor which determines the density profile. Note that since the quantity ξ_w connected with the intrinsic interfacial width and taking into account the definition of ξ_{eff} we may assume that $\xi_{eff}(T_{tr}) > \xi_w(T_{tr})$ as the surface tension includes the capillary wave contribution which increases the value of the surface tension and widens the interfacial profile especially near the triple point. Below we check the validity of eq 45.

APPLICATION TO 2D CASE

The phase coexistence in a two-dimensional fluid system was demonstrated by simulating the liquid–vapor interface of the LJ fluid.⁴⁴ The phenomenon also has found a practical applications within the study of the thermodynamic properties of methane monolayer on the graphite substrate.⁴⁵ Here we apply the results of previous section to the 2D case. For 2D Ising model the exact result for the surface tension σ_{latt} is known from Onsager’s solution:⁴⁶

$$\sigma_{latt}(t) = 2 + t \ln \left(\tanh \frac{1}{t} \right) = 4|\tau| + o(\tau), \quad \tau = 1 - t/t_c \quad (46)$$

This is the expression for the surface tension in longitudinal direction (i.e., along lattice bonds).^{47,48} We use it because the “force” acts in the normal direction to the surface and in such a case the potential J can be related with the amplitude of the LJ-potential which is spherically symmetric. From numerical point of view the difference between surface tension in different direction is insignificant in the region of temperature under consideration.⁴⁹

In view of the Woodbury’s result we can represent eq 46 in a form of eq 21:

$$\sigma_{latt}(t) = t \ln \left(e^{2/t} \tanh \frac{1}{t} \right) = t \ln \left(\frac{\mathcal{A}(m(t))}{\mathcal{A}(-m(t))} \right) \quad (47)$$

where

$$m(t) = \left(1 - \frac{1}{\sinh^4 \frac{2}{t}} \right)^{1/8} \quad (48)$$

The function $\mathcal{A}(m)$ can be decomposed into even and odd parts: $\mathcal{A} = \mathcal{A}_+ + \mathcal{A}_-$, so from eq 47 we derive:

$$\sigma_{latt}(t) = t \ln \left(\frac{1 + \lambda(m(t))}{1 - \lambda(m(t))} \right), \quad \lambda(m) = \mathcal{A}_-(m)/\mathcal{A}_+(m) \quad (49)$$

As we have noted above this result is inconsistent with the Parachore phenomenological approach regardless on the specific choice of the effective exponent a in eq 28. Of course, using eq 47 we can determine \mathcal{A} only up to the arbitrary factor. Elementary algebra gives

$$\lambda(m) = \frac{(1 - \sqrt[4]{1 - m^8})(\sqrt{\sqrt{1 - m^8} + 1} + 1)}{\sqrt{1 - m^8} + \sqrt{\sqrt{1 - m^8} + 1} + 1}$$

and finally we can write

$$\mathcal{A}(m) = \sqrt{1 - m^8} + \sqrt{\sqrt{1 - m^8} + 1} + 1 + \text{sign}(m)(1 - \sqrt[4]{1 - m^8})(\sqrt{\sqrt{1 - m^8} + 1} + 1)$$

According to the relations eq 5 and eq 19 with $z = 1/3$ in the 2D case:²¹

$$\frac{t(T)}{t_c} = 3 \frac{T}{T_* - T} \quad (50)$$

and

$$T_c = T_*/4 = \Phi_0/2 \quad (51)$$

Furthermore, we will use the dimensionless quantities $T \rightarrow T/\Phi_0$ and $n \rightarrow nd^2$. Thus, the isomorphism leads to the following result for the surface tension on the liquid–vapor interface in 2D LJ fluid in the same units as those for the lattice gas:

$$\sigma_{fl}(T) = \sigma_{latt}(t(T)) \quad (52)$$

The corresponding critical behavior of eq 52 is

$$\sigma_{fl}(T) \underset{T \rightarrow T_c - 0}{=} \frac{16}{3}(1 - T/T_c) + \dots \quad (53)$$

The surface tension for the 2D LJ fluid $\sigma_{fl}(T)$ as the function of reduced temperature T/T_c is shown in Figure 1.

Note that the surface tension of the lattice model in eqs 46 and (52) is given in dimensionless units: $\sigma_{latt} = \gamma_{latt} l/J$, where J is the interaction constant of the Ising model.⁴⁶ The surface tension of the LJ fluid is measured in corresponding units: $\sigma_{fl} =$

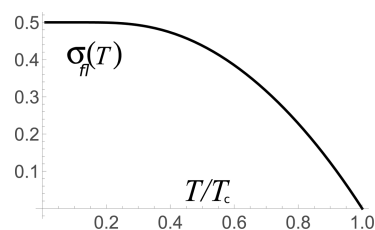


Figure 1. Surface of the 2D Lennard-Jones fluid as the functions of reduced temperature (in units of the critical temperature) according to eqs 46 and 52.

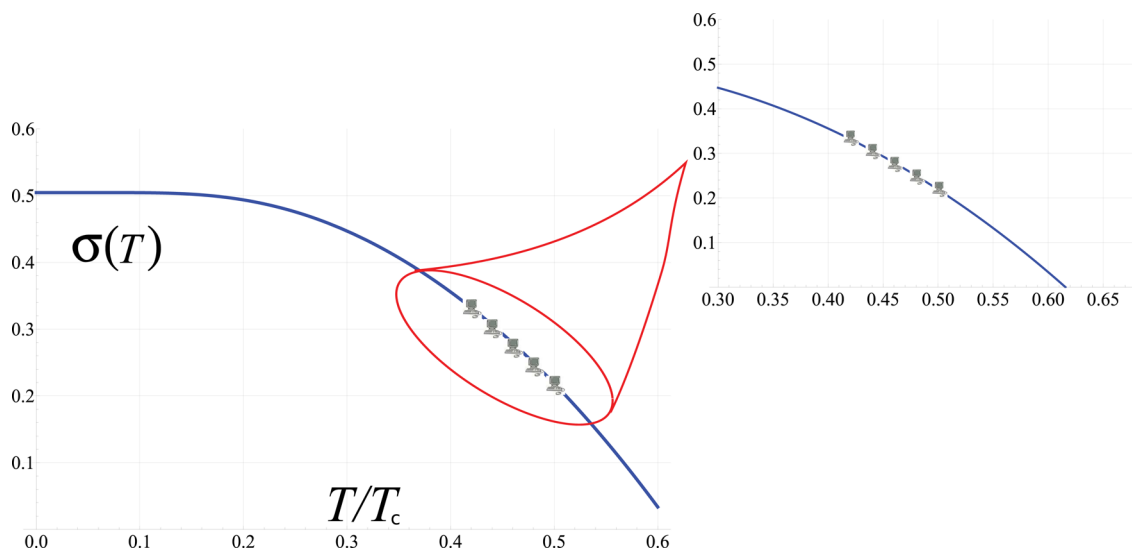


Figure 2. Comparison of the surface tension (eq 52) including (eq 57) with the results of fitting data from ref 50.

$\gamma_{fl}b/\Phi_0$, where Φ_0 and d are the parameters of the LJ potential (11). The simulations of the surface tension for the 2D LJ fluid are scarce and we use the data of the only known to us work of Zeng.⁵⁰ Since the critical temperature for the data in⁵⁰ is not known exactly we use eqs 46, 51, and 52 with the parameters σ_0 and T_* as the fitting parameters in the following expression for the surface tension

$$\sigma_{fl}(T) = \sigma_0 \left(1 + \frac{t(T)}{2} \ln \left(\tanh \frac{1}{t(T)} \right) \right) \quad (54)$$

where $t(T)$ is given by eq 50. The value of σ_0 can be obtained considering the low-temperature asymptote:

$$\lim_{T \rightarrow 0} \sigma_{fl}(T) = \sigma_0 \quad (55)$$

and determines the scale for the surface tension. From the low temperature asymptote of the Onsager's result (eq 46) and eq 13, we obtain

$$\sigma_0 = 2 \frac{J}{\varepsilon} = 0.5 \quad (56)$$

which is consistent with the physical meaning of the surface energy because at $t = 0$ this is exactly the work for a spin to flop. The temperature parameter T_* is related to the critical temperature by eq 51. The least-squares fitting of the data by the expression eq 54 gives the following results

$$\sigma_0 \approx 0.50, \quad T_* \approx 2.46 = 4T_c^{(dat)}, \quad T_c^{(dat)} = 0.615 \quad (57)$$

These values are in good correspondence with theoretical values eq 51 and eq 56. In addition, in the critical point limit $T \rightarrow T_c$ the corresponding slope of $\sigma_{fl}(T)$ is

$$\frac{d\sigma_{fl}}{dT/T_c} \approx -1.346 \quad (58)$$

this value agrees well with eq 53 taking into account relation 13. The result of fitting the data is shown in Figure 2. Note that obtained value for σ_0 also perfectly corresponds to the theoretical estimate (eq 56). This justifies the consistency of our approach.

Now we may use eq 37 in order to determine the effective interfacial thickness ξ_{eff} for LG based on the Bragg-Williams approximation:

$$\xi_{eff} = \left(\frac{\sigma_0}{2} \frac{m(t)}{\sigma(t)} t \ln \frac{1+m(t)}{1-m(t)} \right)^{1/1-\eta}, \quad A = 1/4 \quad (59)$$

Taking into account the relation between temperature variables eq 50 we get the effective thickness for the LJ fluid. Now we compare $\xi_{eff}(t(T))$ with the available data from⁵¹ for the correlation length and the interfacial thickness of the 2D LJ fluid (see Figure 3). It is important that we do not have any fitting

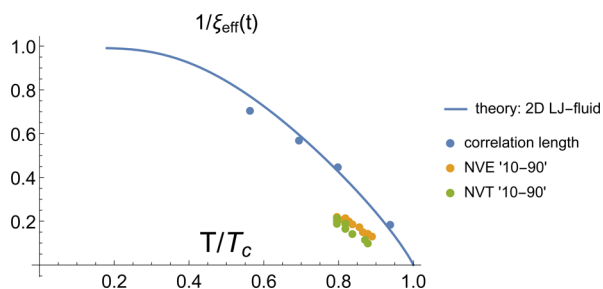


Figure 3. Effective interfacial thickness for 2D LJ fluid from eq 37 and eq 59 with $\sigma_0 = 1/2$, $\eta = 1/4$.

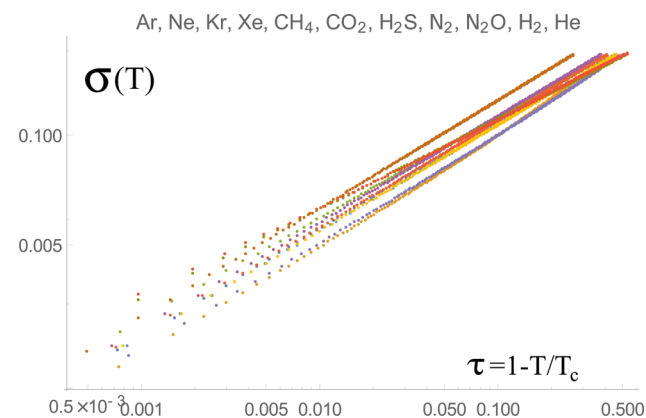


Figure 4. Log–log plot of the surface tension data $\sigma(T)$.

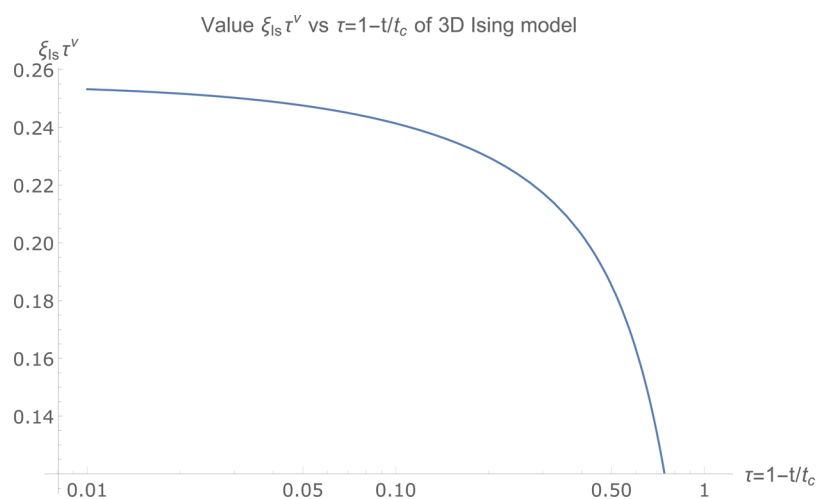


Figure 5. Value $\xi \tau^\nu$, $\nu = 0.625$ for 3D Ising model obtained from low temperature expansion (see ref 58).

Table 1. Effective Critical Exponent ν Obtained by $\sigma \propto \tau^{2\nu}$ -Fitting the Data for the Surface Tension (See Figure 4)

fluid	Ar	Ne	Kr	Xe	CH ₄	CO ₂	H ₂ S	N ₂	H ₂ O	H ₂	He
ν	0.64	0.7	0.65	0.63	0.66	0.64	0.63	0.63	0.63	0.72	0.69

Table 2. Fitting Parameters for the Transformation (Eq 61)

fluid	Ar	Ne	Kr	Xe	CH ₄	CO ₂	H ₂ S	N ₂	H ₂ O	H ₂	He
a	0.08	0.09	0.07	0.08	0.06	0.11	0.06	0.06	0.07	0.08	0.13
$\chi_0 \times 10^{-2}$	-0.3	3.5	-2.0	-0.2	1.1	-0.7	-1.3	-0.9	-0.8	-4.2	-2.0

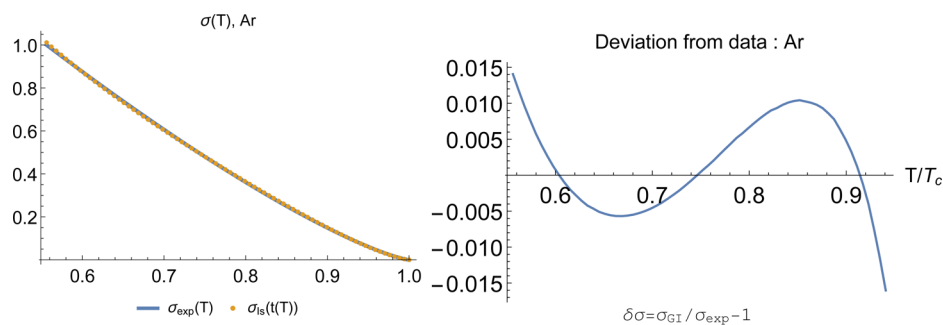


Figure 6. Results for Ar.

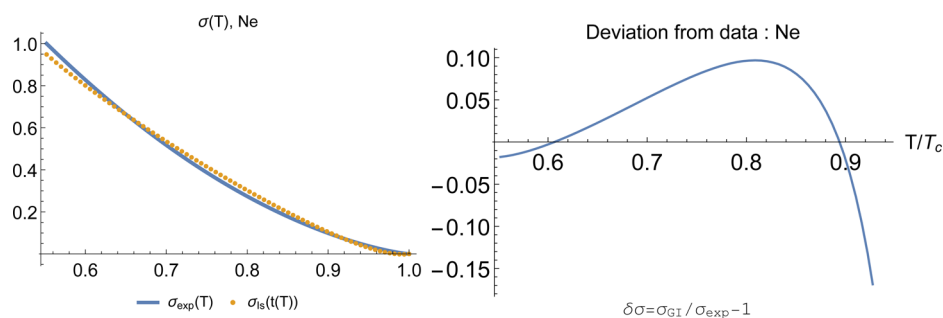


Figure 7. Results for Ne.

parameters in this case because all quantities we get earlier basing solely on the lattice model. The temperature dependencies of the interphase boundary thickness obtained from the NVE- and NVT-simulations according to “10–90” rule⁵² are also presented for comparison. But it appears that only the values of the correlation length⁵¹ fit best to the curve. Bearing in mind that the theoretical curve for the 2D LJ fluid has sense only

in the interval between the triple and the critical points $0.41 < T/\varepsilon < 0.5$.^{53–55} Now we are able to estimate the triple point temperature basing on the inequality (eq 45) and solving the equation $\xi_{eff}(T_{tr}) = 2$. The solution gives the value $T_t \approx 0.38$ which is pretty close to value $T_{tr} \approx 0.41$ obtained in simulations.^{56,57} As we noted above, $\xi_{eff} > \xi_w$ and the estimate based on the approximate equality $\xi_{eff}(T_{tr}) = 2$ indeed

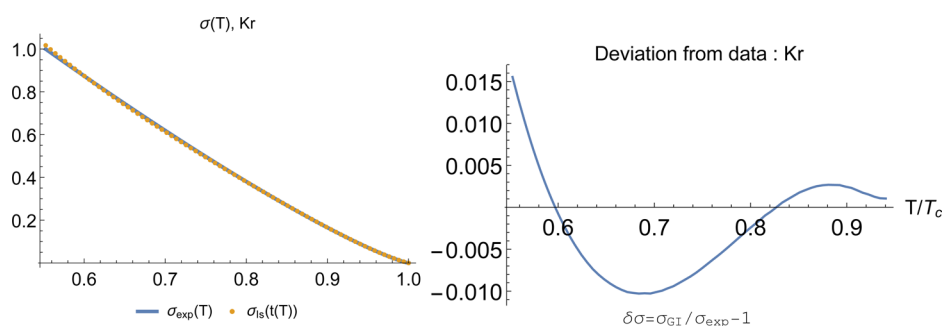


Figure 8. Results for Kr.

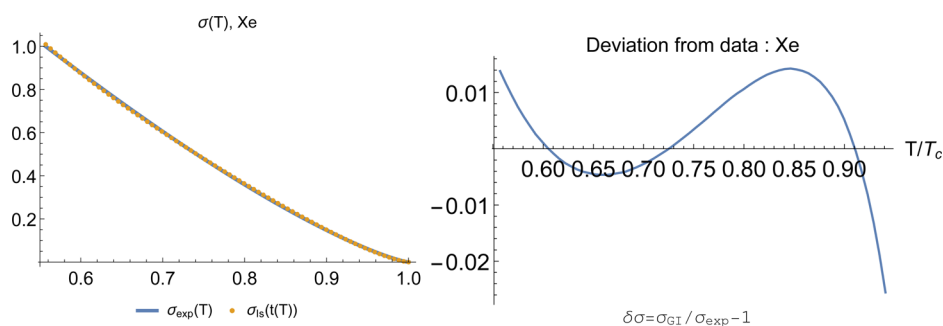
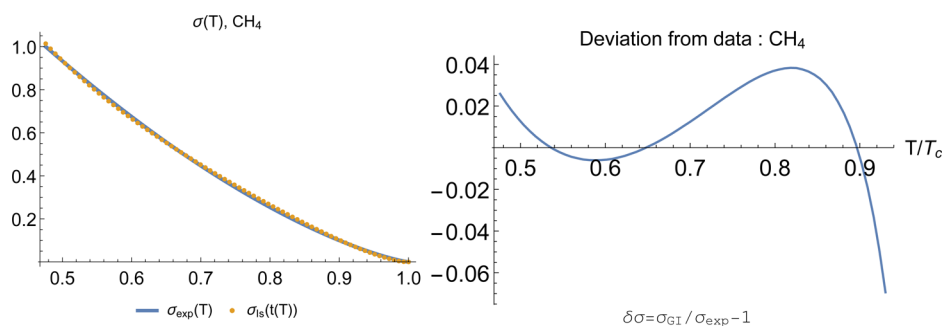
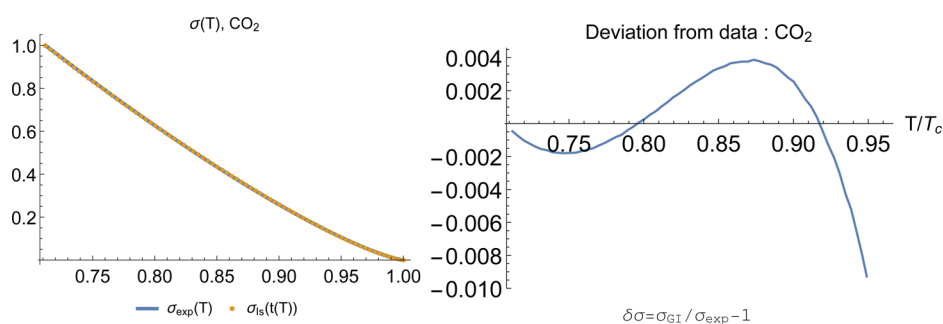


Figure 9. Results for Xe.

Figure 10. Results for CH₄.Figure 11. Results for CO₂.

underestimate the triple point temperature. Based on this result, we see that the correlation length of the isomorphic lattice model can play a role of the effective thickness of the surface for the fluid in eq 37.

APPLICATION TO 3D CASE

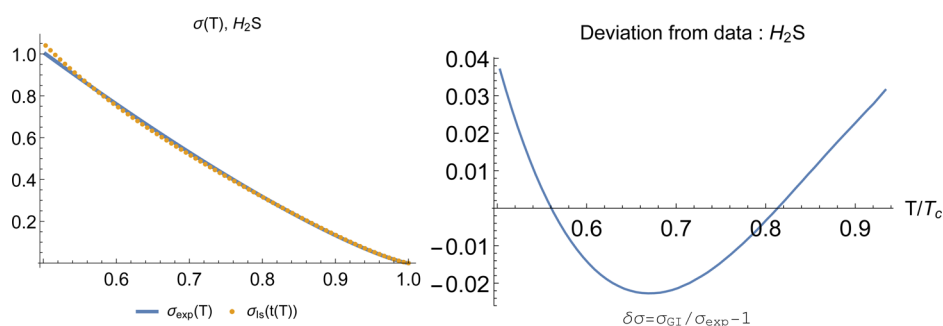
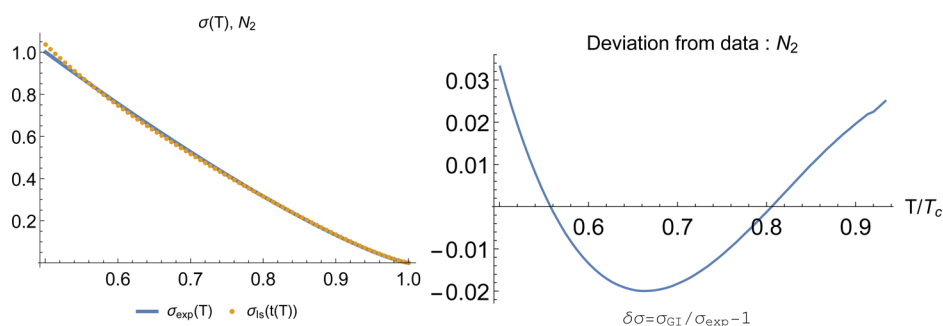
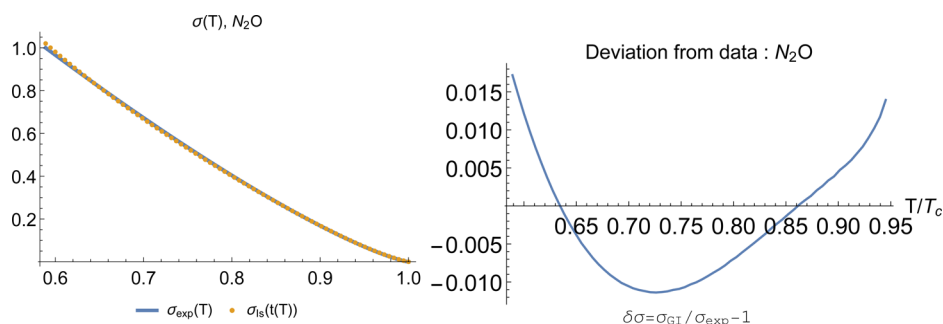
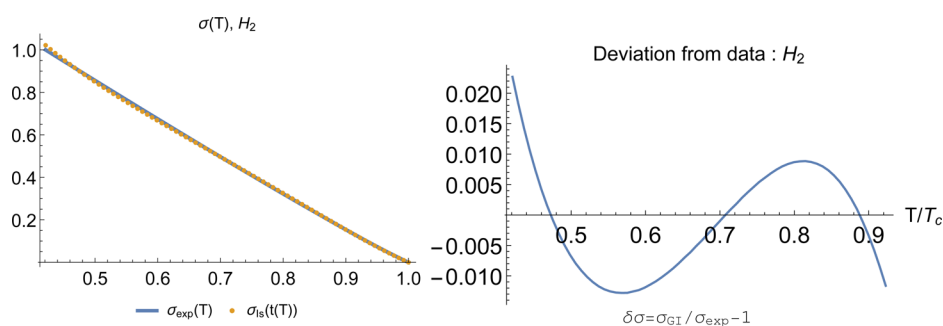
Now we can use the model eq 37 to reproduce the data for the surface tension of the LJ fluid from the information on the binodal. According to eqs 5 and 9 in the 3D case:

$$t(T) = \frac{1}{z} \frac{T}{T_* - T}, \quad z = 1/2, \quad T_* = 4\epsilon$$

and

$$n_* = 3n_c, \quad T_* = 3T_c$$

Substituting these relations as well as the projective transformation for the density (eq 5) into eq 37, we obtain

Figure 12. Results for H₂S.Figure 13. Results for N₂.Figure 14. Results for N₂O.Figure 15. Results for H₂.

$$\sigma/\sigma_{tr} = \frac{\sigma_0}{2\xi_{eff}^{1-\eta}} \frac{t_c}{z} \frac{T/T_*}{(1 - T/T_*)^2} \frac{n_{liq} - n_{gas}}{n_*} \ln \frac{n_{liq}}{n_{gas}} \quad (60)$$

where $n_{liq, gas}$ are the densities of the coexisting phases along the binodal. In contrast to 2D case considered above we do not have universal low temperature asymptotic. We use the value of the surface tension at the triple point $\sigma(T_{tr})$ as a natural scale because of the monotonic increase of $\sigma(T)$ and therefore decrease of $\xi_{eff}(T)$ with lowering the temperature along the

saturation curve. It is important that density dependence in eq 60 is determined by the corresponding approximation for the lattice model and does not use any approximation for the pair correlation function of fluid system.

In order to test our approach in as broad temperature interval and number of substances as possible we use the corresponding NIST data (<http://webbook.nist.gov/chemistry/fluid/>). It is expected that the results based on the global isomorphism approach will be coherent with the data for simple fluids like

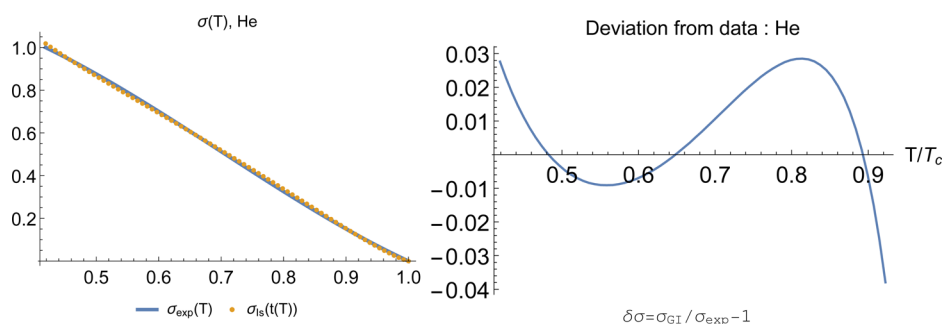
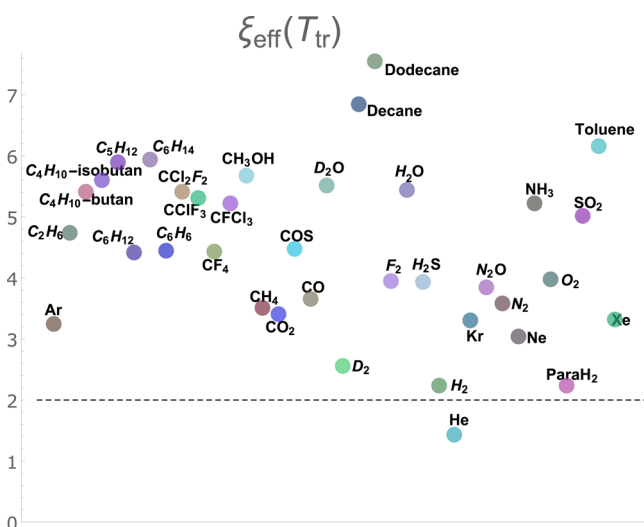


Figure 16. Results for He.

Table 3. Values of $\xi_{\text{eff}}(T_{\text{tr}})$ for the LJ Fluids

fluid	Ar	Ne	Kr	Xe	CH ₄	CO ₂	H ₂ S	N ₂	H ₂ O	H ₂	He
$\frac{\xi_{\text{eff}}(T_{\text{tr}})}{d}$	3.2	3.0	3.3	3.3	3.5	3.4	3.9	3.6	3.8	2.2	1.4

Figure 17. Results for effective thickness $\xi_{\text{eff}}(T_{\text{tr}})$.

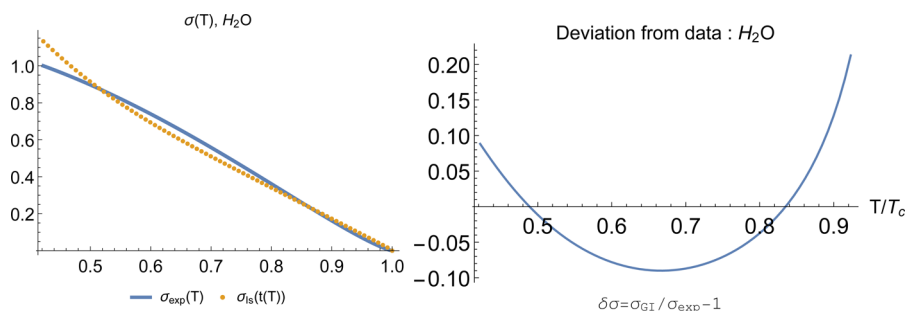
noble gases and CO₂, CH₄ and we demonstrate this below. As follows from the result of the previous section, we identify ξ_{eff} with the correlation length of the Ising model. To test this assumption we use the results of⁵⁸ for the correlation length ξ_{Is} of 3D Ising model based on the low-temperature expansion⁵⁹ in the interval $0.01 \leq 1 - t/t_c \leq 1$ (see Figure 5). This is because the NIST data have greater error in close vicinity of the critical point. This can be seen from the analysis of the scaling behavior $\sigma \propto \tau^{2\nu}$ (see Figure 4 and Table 1). Therefore, we will not analyze the critical asymptotics. Thus, all exponents in eq 37

should be treated as the effective ones rather than the exact asymptotical values.^{60,61}

Now we check the validity of eq 37 along with the assumption that $\xi_{\text{eff}}(T)$ can be directly related to the correlation length of the Ising model in the region of coexistence up to the triple point (see eq 61). With this in mind we put $\eta = 0$ in eq 37. Using the binodal data we determined $\xi_{\text{eff}}(T)$ from eq 37 and now we can compare it with the correlation length of the Ising model. In order to do this we performed additional *homogeneous*, i.e., temperature independent, transformation of the Ising model correlation length ξ_{Is} :

$$\xi_{\text{Is}}^{-1} \rightarrow \xi_{\text{eff}}^{-1}(T) = a \xi_{\text{Is}}^{-1}(t(T)) + \chi_0 \quad (61)$$

The scale parameter a comes from the scale transformation between the spacial scales of the lattice and the fluid. The shift parameter χ_0 takes into account fluctuational shift of the critical point due to inaccuracy of the data which we truncated close to it because of the difference between effective exponent ν in fluid (see Table 1) and $\nu_{\text{Is}} = 0.625$ used in⁵⁸ (see also Figure 5). The corresponding values of a and χ_0 are in Table 2. The results of fitting the surface tension data basing on eqs 37 and 61 are shown in Figure 6–16 along with the corresponding deviations. The value of σ_0 is given by eq 56 as before. As we see for simple fluids which are commonly considered as fluids with LJ type of interaction between particles, the deviations do not exceed 5% in the whole region. Here we note remarkably low deviation (<1%) from the surface tension data for carbon dioxide CO₂. This fluid can be considered as the “canonical” example of the Ising-like fluid not only because of the LJ type of interaction but also due to well-known fact that its crystalline phase has cubic

Figure 18. Results for H₂O.

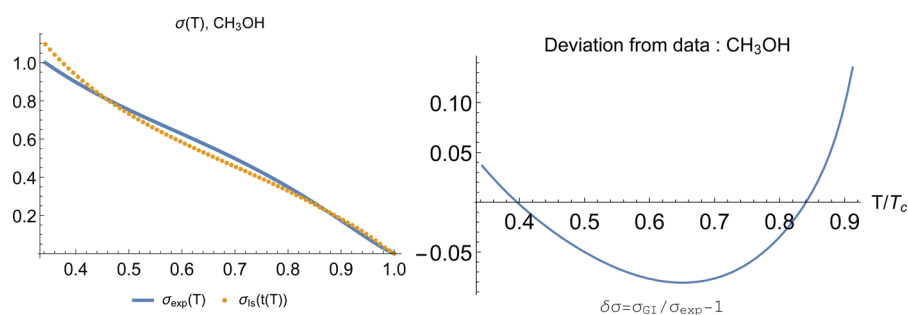
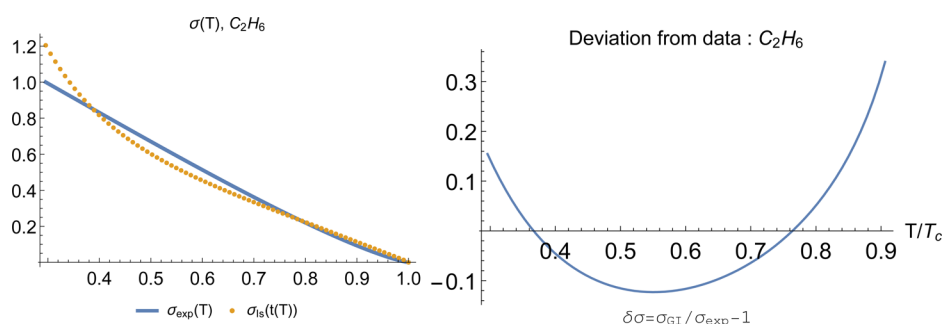
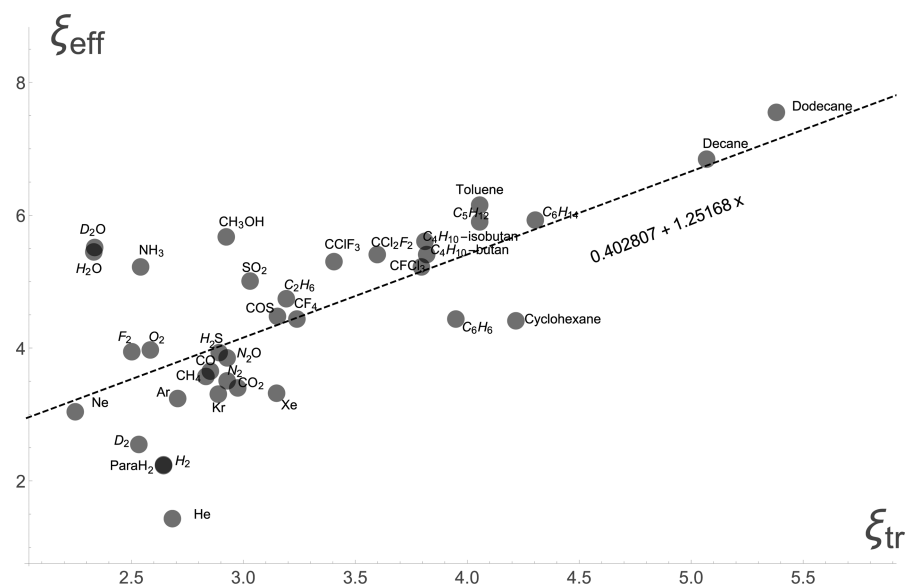
Figure 19. Results for CH₃OH.Figure 20. Results for C₂H₆.

Figure 21. Correlation between $\xi_{\text{eff}}(T_{\text{tr}})$ and the interparticle distance in liquid phase at the triple point $\xi_{\text{tr}} = \left(\frac{3}{4\pi n_l(T_{\text{tr}})}\right)^{1/3}$. The Ising-like LJ-fluids are below the line.

symmetry and therefore it perfectly matches with the cubic Ising model used as the isomorphic lattice model.

Obtained results allow us to analyze the values of the interfacial effective width at the triple point $\xi_{\text{eff}}(T_{\text{tr}})$. For classical LJ-fluids we get $\xi_{\text{eff}}(T_{\text{tr}}) \approx 3\text{--}4 d$ (see Table 3). All of them satisfy the inequality (eq 45) except in case of helium with $\xi_{\text{eff}}(T_{\text{tr}}) \approx 1.43 d$ (see Figure 17). This indicates that the quantum corrections should be taken into account. These values are close to that obtained in square gradient approximation of van der Waals based theories.⁶²

As has been noted above the deviation from spherical symmetry of the interactions is correlated with the greater value

of interfacial width and therefore one can expect that $\xi_{\text{eff}}(T_{\text{tr}}) \gtrsim 4$. Though in such situation the Ising-based model eq 60 becomes inadequate and we can not claim that the values of $\xi_{\text{eff}}(T_{\text{tr}})$ are correct. Indeed, the results of application of Ising model based result for the correlation length in eq 60 for the surface tension of molecular fluids like water, methanol, dodecane ($\xi_{\text{eff}}(T_{\text{tr}}) > 5$) etc. demonstrate much bigger deviations of order 20% (see Figure 18). The Zeno line in water and the binodal diameter have noticeable curvature in low temperature region of triple point.⁶³ Therefore, simple projective transformations (eq 5) are not adequate, and the isomorphic lattice model for such fluids is more complex than

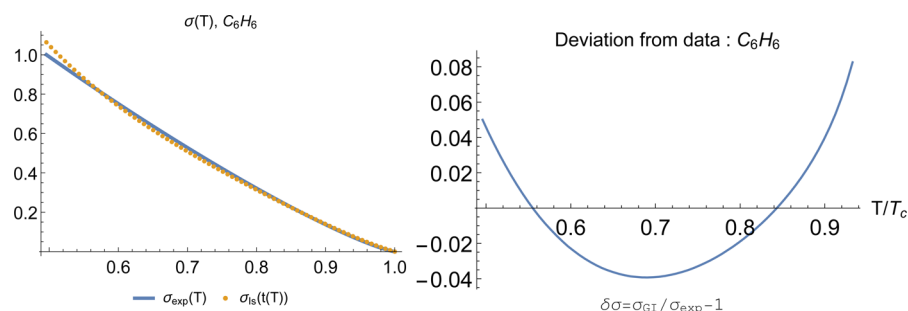
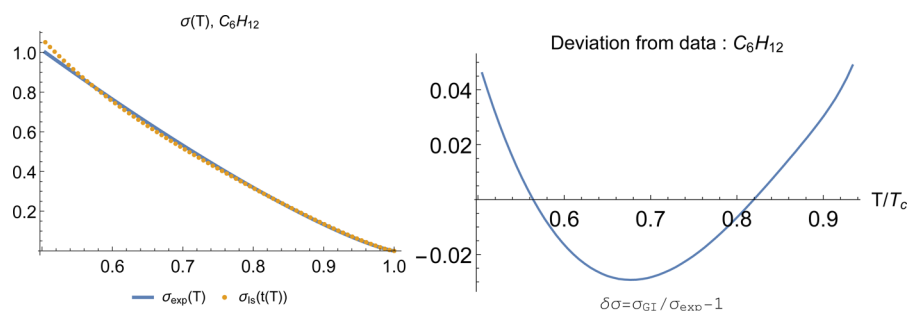


Figure 22. Results for benzene.

Figure 23. Results for C₆H₁₂.Table 4. Values of Mean Error for the LJ Fluids and Corresponding Temperature Interval of Data^a

fluid	mean error, %	interval T/T_c
Ar	0.57	(0.556, 0.940)
Ne	6.0	(0.552, 0.940)
Kr	0.52	(0.553, 0.940)
Xe	0.71	(0.557, 0.941)
CH ₄	1.78	(0.475, 0.930)
CO ₂	0.28	(0.712, 0.962)
H ₂ S	1.57	(0.503, 0.934)
N ₂	1.37	(0.50, 0.933)
C ₆ H ₁₂	2.06	(0.505, 0.934)
C ₆ H ₆	2.8	(0.496, 0.933)
N ₂ O	0.71	(0.589, 0.945)
H ₂	0.75	(0.421, 0.923)
He	1.34	(0.419, 0.923)

^aThe number of data points in the interval is 66.

standard Ising model. This is because the orientational correlations are essential for such fluids and simple Ising model is not adequate isomorphic lattice model in such cases (see also ref 64). Results for CH₃OH and C₂H₆ are given in Figures 19 and 20.

It is interesting to compare $\xi_{eff}(T_{tr})$ with another characteristic scale—the average distance between particles in liquid phase:

$$\xi_{tr} = \left(\frac{3}{4\pi n_l(T_{tr})} \right)^{1/3}$$

The correlation between $\xi_{eff}(T_{tr})$ and ξ_{tr} is shown in Figure 21. It demonstrates that Ising-like fluids are separated from more complex ones (above the dashed line). As it is clear from Figure 21 for fluids like water, methanol and ammonia where orientational correlations due to hydrogen bonds are essential the ratio takes greater values. Also we see that in addition to

standard simple fluids there are two fluids benzene C₆H₆ and cyclohexane C₆H₁₂ which are characterized shorter value of $\xi_{eff}(T_{tr})$ than other liquids with the same value of ξ_{tr} . These two fluids demonstrate rather good correspondence between Ising based model eq 60 and the data (see Figures 22 and 23).

Obviously, only when the contribution of orientational degrees of freedom is negligible then the isotropic Ising model could serve as the valid isomorphic lattice model. Pitzer's acentric factor ω is commonly used as the measure of non sphericity.⁶⁵ In refs 24 and 66, it was demonstrated how to include ω into the global isomorphism approach. Because ω is defined phenomenologically now we can not relate it with some parameter of the isomorphic lattice model. This would allow to extend the approach for the case of fluids with short linear Lennard-Jones chains as their surface tension follows the universal argon-like behavior according to the results of Galliero et. al.⁴⁰

We note also that our results for C₆H₁₂ (hexane) and N₂ are comparable in errors (see Table 4) with the results of⁶⁷ where the semiempirical equations, which include Pitzer's acentric factor, were used.

CONCLUSION

As a summary, we have demonstrated that the global isomorphism approach based on simplest form of the projective transformations eq 5 can be applied not only for the study of the bulk properties of coexisting phases but also for the description of the surface tension. This suggests that thermodynamic properties in the Lennard-Jones type fluids can be obtained on the basis of the information about the Ising model. In particular, the interfacial width is related with the correlation length of the Ising model below the critical point. Thus, there is no ambiguity connected with the difference in correlation lengths of the coexisting phases because the restoration of symmetry of phase coexistence. The unification of thermodynamic properties as well as the surface tension along the saturation curve for simple fluids⁶⁸ is quite natural within such an approach. We have

improved Woodbury's original approach²³ in order to get the correct critical asymptotics for the surface tension via introducing the effective width of the interface $\xi_w(T)$ on the basis of the Ornstein–Zernike equation. From simple physical consideration it follows that at the triple point $\xi_w(T_{tr}) \gtrsim 2$. This corresponds quite well with the known results for this value defined using the specific forms of the density profile. Here the results of computer simulations of density profile and surface tension in Mie($n-6$) fluids as well as their n -dependence³⁹ can be used to test the relation between the correlation length of the Ising model and the interfacial width proposed here.

Using global isomorphism, we relate this value with the correlation length of the Ising model thus avoiding the difficulty with the existence of two correlation length for liquid–vapor equilibrium. Our approach gives good results for “classical” LJ fluids like noble gases and carbon dioxide with almost perfect spherical symmetry of the particle and their interactions. Clearly it becomes inadequate for more complex fluids like water and butan. Although the general algorithm for constructing the isomorphic lattice model for a given class of fluids is not known some basic physical reasonings like critical compressibility factor value (see ref 64) and topological equivalence of the phase diagrams are the guides to build relevant isomorphic lattice Ising-like models for complex fluids. Sure it is possible to use more sophisticated approaches for calculating the lattice model to include the fluctuations of the mean-field. On the basis of the obtained results we can expect that near the critical point all approximations will lead to the same critical behavior (eq 36). Taking into account fluctuations using the relevant approximation for Woodbury parameter s in eq 22 is the natural way of improvement.

The existence of exact results for lattice models is of great importance for testing the global isomorphism approach. For example, one may speculate about the analog of the Kramers–Wannier symmetry^{15,69} for 2D LJ fluid as the replica of the corresponding symmetry of 2D Ising model due to global isomorphism. In such a case, there must be correspondence between the thermodynamic properties along the binodal median above and below critical point. This intriguing direct consequence of the global isomorphism can be tested in computer simulations.

Another important issue related to the surface tension, the particle-hole symmetry and the linearity of the binodal diameter is the Tolman length δ_T .⁷⁰ It is well-known that this finite size correction to the surface tension vanishes for the symmetrical models.^{71–73} In ref 74, it was suggested that the Tolman length is related to the density diameter at the phenomenological level. Within the global isomorphism approach, this means that it is possible to relate the Tolman length to the asymmetry parameter z explicitly. This also will be the subject of the future work.

AUTHOR INFORMATION

Corresponding Author

*(V.L.K.) E-mail: kulinskij@onu.edu.ua. Telephone: +38(0) 487317556.

Notes

The authors declare no competing financial interest.

ACKNOWLEDGMENTS

This work is partially supported by Ministry of Education and Science of Ukraine, Grant No 0115U003214. V.L.K. also

acknowledges Mr. Konstantin Yun for continuous support of the research. The help of Mrs. S. Bogdan in reviewing the text of the manuscript is kindly appreciated.

REFERENCES

- (1) van der Waals, J. D. *De Continuïtet van den Gas - En Floeistoetstand*. Ph.D. thesis, Leiden University, Leiden, 1873.
- (2) Pitzer, K. S. *Corresponding States for Perfect Liquids*. *J. Chem. Phys.* **1939**, *7*, 583–590.
- (3) Cailletet, L.; Mathias, E. *Seances Acad. Sci.* **1886**, *102*, 1202.
- (4) Guggenheim, E. A. *The Principle of Corresponding States*. *J. Chem. Phys.* **1945**, *13*, 253–261.
- (5) Frenkel, D.; Smit, B. *Understanding Molecular Simulation, Second ed.: From Algorithms to Applications (Computational Science Series, Vol 1)*; 2nd ed.; Academic Press: 2001; p 658.
- (6) Ross, M.; Hensel, F. A Modified Van der Waals Model for the Coexistence Curve of Expanded Metals. *J. Phys.: Condens. Matter* **1996**, *8*, 1909–1919.
- (7) Ben-Amotz, D.; Herschbach, D. R. Correlation of Zeno ($Z = 1$) Line for Supercritical Fluids with Vapor-Liquid Rectilinear Diameter. *Isr. J. Chem.* **1990**, *30*, 59–68.
- (8) Batschinski, A. Abhandlungen über Zustandgleichung; Abh. I: Der orthometrische Zustand; *Ann. Phys.* **1906**, *324*, 307–309.
- (9) Apfelbaum, E. M.; Vorob'ev, V. S. A New Similarity Found from the Correspondence of the Critical and Zeno-Line Parameters. *J. Phys. Chem. B* **2008**, *112*, 13064–13069.
- (10) Apfelbaum, E. M.; Vorob'ev, V. S. The Confirmation of the Critical Point-Zeno-Line Similarity Set from the Numerical Modeling Data for Different Interatomic Potentials. *J. Chem. Phys.* **2009**, *130*, 214111.
- (11) Apfelbaum, E. M.; Vorob'ev, V. S. Correspondence between the Critical and the Zeno-Line Parameters for Classical and Quantum Liquids. *J. Phys. Chem. B* **2009**, *113*, 3521–3526.
- (12) Kulinskii, V. L. Simple Geometrical Interpretation of the Linear Character for the Zeno-Line and the Rectilinear Diameter. *J. Phys. Chem. B* **2010**, *114*, 2852–2855.
- (13) Kulinskii, V. L. Global Isomorphism Between the Lennard-Jones Fluids and the Ising Model. *J. Chem. Phys.* **2010**, *133*, 034121.
- (14) Bulavin, L. A.; Kulinskii, V. L. Unified Picture for the Classical Laws of Batschinski and the Rectilinear Diameter for Molecular Fluids. *J. Phys. Chem. B* **2011**, *115*, 6061–6068.
- (15) Baxter, R. J. *Exactly Solved Models in Statistical Mechanics*; Dover: New York, 2007.
- (16) Okumura, H.; Yonezawa, F. Liquid-Vapor Coexistence Curves of Several Interatomic Model Potentials. *J. Chem. Phys.* **2000**, *113*, 9162–9168.
- (17) Duda, Y.; Romero-Martinez, A.; Orea, P. Phase Diagram and Surface Tension of the Hard-Core Attractive Yukawa Model of Variable Range: Monte Carlo Simulations. *J. Chem. Phys.* **2007**, *126*, 224510.
- (18) Orea, P.; Duda, Y. On the Corresponding States Law of the Yukawa Fluid. *J. Chem. Phys.* **2008**, *128*, 134508.
- (19) Landau, L. D.; Lifshitz, E. M. *Statistical Physics (Part 1)*, 3rd ed.; Pergamon Press: Oxford, 1980.
- (20) Huang, K. *Statistical Mechanics*, 2nd ed.; Wiley: 1987.
- (21) Kulinskii, V. L. Communication: The Application of the Global Isomorphism to the Study of Liquid-Vapor Equilibrium in Two and Three-Dimensional Lennard-Jones Fluids. *J. Chem. Phys.* **2010**, *133*, 131102.
- (22) Chandler, D. *Introduction to Modern Statistical Mechanics*; Oxford University Press: 1987.
- (23) Woodbury, G. W. J. General Equation for the Surface Tension of the Lattice Gas. *J. Chem. Phys.* **1969**, *51*, 1231–1235.
- (24) Kulinskii, V. L. The Critical Compressibility Factor of Fluids from the Global Isomorphism Approach. *J. Chem. Phys.* **2013**, *139*, 184119.
- (25) Bulavin, L.; Cheplak, V.; Kulinskii, V. In *Physics of Liquid Matter: Modern Problems*; Bulavin, L., Lebovka, N., Eds.; Springer Proceedings

in Physics; Springer International Publishing: 2015; Vol. 171; pp 53–75.

(26) Liu, A. J.; Fisher, M. E. The Three-Dimensional Ising Model Revisited Numerically. *Phys. A* **1989**, *156*, 35–76.

(27) Domb, C.; Sykes, M. F. On Metastable Approximations in Cooperative Assemblies. *Proc. R. Soc. London, Ser. A* **1956**, *235*, 247–259.

(28) Sanchez, I. C.; Boening, K. L. Universal Thermodynamics at the Liquid-Vapor Critical Point. *J. Phys. Chem. B* **2014**, *118*, 13704–13710.

(29) Hansen, J.-P.; McDonald, I. R. *Theory of Simple Liquids*, Third Edition; Academic Press, 2006; p 428.

(30) Binder, K. Simulations of Interfacial Phenomena in Soft Condensed Matter and Nanoscience. *J. Phys.: Conf. Ser.* **2014**, *510*, 012002.

(31) Woodbury, G. W. J. Surface Tension in Lattice Models. *J. Chem. Phys.* **1970**, *53*, 3728–3732.

(32) Woodbury, G. W. J. Surface Tension Calculations for the Hard Square Lattice Gas. *J. Chem. Phys.* **1972**, *57*, 847–851.

(33) Rowlinson, J.; Widom, B. *Molecular Theory of Capillarity*; Clarendon Press: Oxford, U.K., 1982; p 352.

(34) Widom, B. Surface Tension and Molecular Correlations near the Critical Point. *J. Chem. Phys.* **1965**, *43*, 3892–3897.

(35) Fisk, S.; Widom, B. Structure and Free Energy of the Interface Between Fluid Phases in Equilibrium near the Critical Point. *J. Chem. Phys.* **1969**, *50*, 3219–3227.

(36) Fisher, I. Z. *Statistical Theory of Liquids*; University of Chicago Press: 1964.

(37) Blokhuis, E.; Bedeaux, D.; Holcomb, C.; Zollweg, J. Tail Corrections to the Surface Tension of a Lennard-Jones Liquid-Vapor Interface. *Mol. Phys.* **1995**, *85*, 665–669.

(38) Macleod, D. B. On a Relation Between Surface Tension and Density. *Trans. Faraday Soc.* **1923**, *19*, 38–41.

(39) Galliero, G.; Piñeiro, M. M.; Mendiboure, B.; Miqueu, C.; Lafitte, T.; Bessieres, D. Interfacial Properties of the Mie $n - 6$ Fluid: Molecular Simulations and Gradient Theory Results. *J. Chem. Phys.* **2009**, *130*, 104704.

(40) Galliero, G. Surface Tension of Short Flexible Lennard-Jones Chains: Corresponding States Behavior. *J. Chem. Phys.* **2010**, *133*, 074705.

(41) Triezenberg, D. G.; Zwanzig, R. Fluctuation Theory of Surface Tension. *Phys. Rev. Lett.* **1972**, *28*, 1183–1185.

(42) Schofield, P. The Statistical Theory of Surface Tension. *Chem. Phys. Lett.* **1979**, *62*, 413–415.

(43) Lekner, J.; Henderson, J. R. Theoretical Determination of the Thickness of a Liquid-Vapor Interface. *Phys. A* **1978**, *94*, 545–558.

(44) Abraham, F. F. Evidence for Two-Dimensional Liquid-Vapor Coexistence: A Monte Carlo Computer Simulation. *J. Chem. Phys.* **1980**, *72*, 1412–1413.

(45) Jiang, S.; Gubbins, K. E. Vapour-Liquid Equilibria in Two-Dimensional Lennard-Jones Fluids: Unperturbed and Substrate-Mediated Films. *Mol. Phys.* **1995**, *86*, 599–612.

(46) Onsager, L. Crystal Statistics. I. A Two-Dimensional Model with an Order-Disorder Transition. *Phys. Rev.* **1944**, *65*, 117–149.

(47) Fisher, M. E.; Ferdinand, A. E. Interfacial, Boundary, and Size Effects at Critical Points. *Phys. Rev. Lett.* **1967**, *19*, 169–172.

(48) Rottman, C.; Wortis, M. Exact Equilibrium Crystal Shapes at Nonzero Temperature in Two Dimensions. *Phys. Rev. B: Condens. Matter Mater. Phys.* **1981**, *24*, 6274–6277.

(49) Hunter, J. E.; Reinhardt, W. P. Finite-Size Scaling Behavior of the Free Energy Barrier Between Coexisting Phases: Determination of the Critical Temperature and Interfacial Tension of the Lennard-Jones Fluid. *J. Chem. Phys.* **1995**, *103*, 8627–8637.

(50) Zeng, X. C. Gas-Liquid Nucleation in Two-Dimensional Fluids. *J. Chem. Phys.* **1996**, *104*, 2699–2704.

(51) Mederos, L.; Chacon, E.; Navascues, G.; Lombardero, M. Two-Dimensional Lennard-Jones Liquid-Vapor Interphase. A Functional Perturbation Approach. *Mol. Phys.* **1985**, *54*, 211–224.

(52) Chen, L.-J.; Robert, M.; Shukla, K. P. Molecular Dynamics Study of the Temperature Dependence of the Interfacial Thickness in Two-Dimensional Fluid Phases. *J. Chem. Phys.* **1990**, *93*, 8254–8259.

(53) Abraham, F. F. The Phases of Two-Dimensional Matter, Their Transitions, and Solid-State Stability: A Perspective via Computer Simulation of Simple Atomic Systems. *Phys. Rep.* **1981**, *80*, 340–374.

(54) Smit, B.; Frenkel, D. Vapor-Liquid Equilibria of the Two-Dimensional Lennard-Jones Fluid(s). *J. Chem. Phys.* **1991**, *94*, 5663–5668.

(55) Tang, J.; Ge, G.; Brus, L. E. Gas-Liquid-Solid Phase Transition Model for Two-Dimensional Nanocrystal Self-Assembly on Graphite. *J. Phys. Chem. B* **2002**, *106*, 5653–5658.

(56) Barker, J.; Henderson, D.; Abraham, F. Phase Diagram Of the Two-Dimensional Lennard-Jones System; Evidence For First-Order Transitions. *Phys. A* **1981**, *106A*, 226–238.

(57) Phillips, J. M.; Bruch, L. W.; Murphy, R. D. The Two-Dimensional Lennard-Jones System: Sublimation, Vaporization, and Melting. *J. Chem. Phys.* **1981**, *75*, 5097–5109.

(58) Hasenbusch, M.; Pinn, K. Surface Tension, Surface Stiffness, and Surface width of the 3-Dimensional Ising Model on a Cubic Lattice. *Phys. A* **1993**, *192*, 342–374.

(59) Arisue, H.; Fujiwara, T. High Order Calculation of the Strong Coupling Expansion for the Mass Gap in Lattice Gauge Theory. *Nucl. Phys. B* **1987**, *285*, 253–263.

(60) Kouvel, J. S.; Fisher, M. E. Detailed Magnetic Behavior of Nickel Near its Curie Point. *Phys. Rev.* **1964**, *136*, A1626–A1632.

(61) Anisimov, M. A.; Kiselev, S. B.; Sengers, J. V.; Tang, S. Crossover Approach to Global Critical Phenomena in Fluids. *Phys. A* **1992**, *188*, 487–525.

(62) Lu, B. Q.; Evans, R.; Telo da Gama, M. The Form of the Density Profile at a Liquid-Gas Interface. Dependence on the Intermolecular Potential. *Mol. Phys.* **1985**, *55*, 1319–1338.

(63) Reagan, M. T.; Tester, J. W. The Zeno ($Z = 1$) Behavior of Water: A Molecular Simulation Study. *Int. J. Thermophys.* **2001**, *22*, 149–160.

(64) Kulinskii, V. L. The Critical Compressibility Factor Value: Associative Fluids and Liquid Alkali Metals. *J. Chem. Phys.* **2014**, *141*, 054503.

(65) Pitzer, K. S.; Curl, R. F. The Volumetric and Thermodynamic Properties of Fluids. III. Empirical Equation for the Second Virial Coefficient. *J. Am. Chem. Soc.* **1957**, *79*, 2369–2370.

(66) Wei, Q.; Herschbach, D. R. Isomorphism in Fluid Phase Diagrams: Kulinskii Transformations Related to the Acentric Factor. *J. Phys. Chem. C* **2013**, *117*, 22438–22444.

(67) Garrido, J. M.; Mejia, A.; Pineiro, M. M.; Blas, F. J.; Müller, E. A. Interfacial Tensions of Industrial Fluids from a Molecular-Based Square Gradient Theory. *AIChE J.* **2016**, *15190*.

(68) Yi, H.; Tian, J. Corresponding states correlation for temperature dependent surface tension of normal saturated liquids. *Int. J. Mod. Phys. B* **2014**, *28*, 1450169.

(69) Kramers, H. A.; Wannier, G. H. Statistics of the Two-Dimensional Ferromagnet. Part I. *Phys. Rev.* **1941**, *60*, 252–262.

(70) Tolman, R. C. The Effect of Droplet Size on Surface Tension. *J. Chem. Phys.* **1949**, *17*, 333–337.

(71) Fisher, M. P. A.; Wortis, M. Curvature Corrections to the Surface Tension of Fluid Drops: Landau Theory and a Scaling Hypothesis. *Phys. Rev. B: Condens. Matter Mater. Phys.* **1984**, *29*, 6252–6260.

(72) van Giessen, A. E.; Blokhuis, E. M.; Bukman, D. J. Mean Field Curvature Corrections to the Surface Tension. *J. Chem. Phys.* **1998**, *108*, 1148–1156.

(73) Kulinskii, V. L. Asymmetry of the Hamiltonian and the Singular Behavior of the Tolman Length within the Canonical Formalism Approach. *Ukr. J. Phys.* **2015**, *60*, 845–854.

(74) Anisimov, M. A. Divergence of Tolman's Length for a Droplet near the Critical Point. *Phys. Rev. Lett.* **2007**, *98*, 035702.